Bull. Mater. Sci., Vol. 28, No. 7, December 2005, pp. 651–661. © Indian Academy of Sciences.

Pressure dependence of elastic properties of ZnX (X = Se, S and Te): Role of charge transfer

DINESH VARSHNEY*, P SHARMA, N KAURAV and R K SINGH[†]

School of Physics, Vigyan Bhawan, Devi Ahilya University, Khandwa Road Campus, Indore 452 017, India
[†]Lakshmi Narayan College of Technology, Raisen Road, Bhopal 462 021, India

MS received 1 March 2005; revised 15 October 2005

Abstract. An effective interaction potential (EIOP) is developed to invoke the pressure induced phase transition from zinc blende (*B*3) to rocksalt (*B*1) structure and anharmonic properties in ZnX (X = Se, S, Te) semiconductors. The effective interaction potential incorporates the long range Coulomb interaction, van der Waals interaction and short-range repulsive interaction up to second neighbour ions within the Hafemeister and Flygare approach as well as the charge transfer effects caused by the electron-shell deformation of the overlapping ions. The van der Waals coefficients are computed by the Slater Kirkwood variation method as a first step. Later on, we evaluate volume collapse, second order and third order elastic constants with pressure pointing to the systematic trends in all compounds of zinc blende structure and their thermal properties such as force constant, Gruneisen parameter, compressibility, Debye temperature etc. The vast volume discontinuity in pressure–volume (PV) phase diagram identifies the structural phase transition from zinc blende (*B*3) to rock salt (*B*1) structure and is consistent with those revealed from earlier reports.

Keywords. Phase transition; elastic constants; thermodynamical properties.

1. Introduction

The quest for the nature of interatomic interactions in solids is of paramount importance as it leads to an understanding of their thermodynamical, elastic and numerous other physical properties. Pressure is identified as an attractive thermodynamical variable to reveal the mechanical properties of most of the solids and alloys. In recent years there has been considerable interest in theoretical and experimental studies of $A^N B^{8-N}$ type crystals with zinc blende structure. It is attributed to their high symmetry and simplicity of their ionic bonding (Mujica *et al* 2003). Almost all the A^{II}–B^{VI} compounds crystallize either in the zinc blende or wurtzite structures. The common and dominant feature of these structures is the tetrahedral bonding to four atoms of the other elements. In zinc blende these tetrahedral are arranged in a cubic type structure whilst they are in a hexagonal type structure. Indeed, the centres of similar tetrahedral are arranged in a face-centred cubic (*fcc*) array in the former and a hexagonal closed-packed (*hcp*) array in the latter (Jain 1991).

Quite generally at a particular pressure, A^{II}–B^{VI} compounds (herein after ZnX system) are known to undergo a first-order phase-transition from the *B*3 to *B*1 as observed in diamond cell by optical (polarized light) and IR microscopy measurement (Piermarini and Block 1975). Arora and coworkers (1988) reported the results of a detailed Raman scattering investigation of the zone-centre optical phonons of the mixed crystal, $Zn_xMn_{1-x}Se$ ($0 \le x \le 0{\cdot}33$). In the earlier past, there was an extensive theoretical study and understanding of phase-transition and anharmonic properties of solids by means of different forms of cohesion.

The major part of cohesion in these potentials is contributed by long-range Coulomb interactions, which are counter balance, by the short-range overlap repulsion owing its origin to the Pauli exclusion principle. Born and Mayer (1932) employed overlap repulsion with a lattice sum to describe the cohesion in most of ionic solids. We refer to an earlier work of Tosi and Fumi (1962) and Tosi (1964) who properly incorporated van der Waals interaction along with *d*–*d* (r^{-6}) and *d*–*q* (r^{-8}) interactions to reveal the cohesion in several ionic solids. We also quote the work of Singh (1982), who introduced the effects of charge transfer i.e. three-body interactions and followed Hafemeister and Flygare (1965) type overlap repulsion up to second neighbour ions besides short range interactions to discuss the mechanical properties of several solids and alloys. Despite their successes, the basic nature of these interatomic potentials is such that they are inadequate to reveal a consistent picture of the interaction mechanism in ionic solids.

The present investigation is organized as follows. We begin with the estimation of van der Waals coefficient from the Slater–Kirkwood variational method with an idea that both the ions are polarizable. Later on, the phase transition pressures and elastic constants are deduced within the framework of the Shell model, that incorporates the long-range Coulomb, van der Waals (vdW) interaction, the short range overlap repulsive interaction up

*Author for correspondence (vdinesh33@rediffmail.com)

to second neighbour ions within the Hafemeister and Flygare approach and the three-body interaction. The computed results and numerical analysis are discussed in § 3. We aimed at how by minimizing Gibbs free energies of both the phases we trace the results. The results obtained from this method and their comparison with experimental results are presented in § 4.

2. The model

It is well known that pressure causes a change in the volume of the crystal and consequently it alters the charge distribution of the electron shells. As a result of this, a deformation of the overlapping shell takes place that gives rise to charge transfer (or three-body interaction) effects. We begin by writing the Gibbs-free energy

$$G = U + PV - TS, \tag{1}$$

to obtain the structural stability condition for a crystal for a particular lattice spacing, r. Here U is the internal energy, which at 0 K corresponds to the cohesive energy, S the vibrational entropy at absolute temperature, T, at 0 K, pressure, P and the volume, V. The Gibbs free energy for zinc blende [ZB] structure ($B3$, real) and rocksalt [RS] ($B1$, hypothetical) structure is given by

$$G_{B3}(r) = U_{B3}(r) + 3{\cdot}08Pr^3, \tag{2}$$

$$G_{B1}(r') = U_{B1}(r') + 2{\cdot}00Pr'^3, \tag{3}$$

with $U_{B3}(r)$ and $U_{B1}(r')$ as the lattice energies for ZB and RS structures. The internal energy consists of the long range Coulomb, modified three-body interaction (Singh 1982), the short-range van der Waals interaction and overlap repulsion effective up to the second neighbour ions. Their relevant expressions are written as

$$\begin{aligned} U_{B3}(r) = &-\frac{a_{\mathrm{M}} Z^2 e^2}{r} - \frac{4a_{\mathrm{m}} Ze^2}{r} f(r) \\ &- \sum_{ij} \frac{C_{ij}}{r_{ij}} - \sum_{ij} \frac{D_{ij}}{r_{ij}} + b\sum_{ij} b_{ij} \exp\left(\frac{r_i + r_j - r_{ij}}{r}\right) \\ &+ b\sum_{ii} b_{ii} \exp\left(\frac{2r_i - kr_{ij}}{r}\right) + b\sum_{jj} b_{jj} \exp\left(\frac{2r_j - kr_{ij}}{r}\right), \end{aligned} \tag{4}$$

$$\begin{aligned} U_{B1}(r') = &-\frac{a'_{\mathrm{M}} Z^2 e^2}{r'} - \frac{4a'_{\mathrm{M}} Ze^2}{r} f(r') \\ &- \sum_{ij} \frac{C'_{ij}}{r'_{ij}} - \sum_{ij} \frac{D'_{ij}}{r'_{ij}} + b\sum_{ij} b_{ij} \exp\left(\frac{r_i + r_j - r'_{ij}}{r}\right) \\ &+ b\sum_{ii} b_{ii} \exp\left(\frac{2r_i - k'r'_{ij}}{r}\right) + b\sum_{jj} b_{jj} \exp\left(\frac{2r_j - k'r'_{ij}}{r}\right), \end{aligned} \tag{5}$$

with a_{M} and a'_{M} as the Madelung constants for ZB (RS) structure, respectively. C_{ij} and D_{ij} are overall van der Waals coefficient, b_{ij} (i, j = 1,2) are Pauling coefficients, Ze the ionic charge, b (r) the range (hardness) parameters, r (r') the nearest neighbour separations for ZB (RS) structures, f (r) the three-body force parameters and k(k') the structure factor for $B3$ and $B1$ phases.

The study of the second order elastic constants (SOEC) [C_{11}, C_{12}, C_{22}], the third order elastic constants (TOEC) [C_{111}, C_{112}, C_{123}, C_{144}, C_{166}, C_{456}] and their pressure derivatives at 0 K is quite important for understanding the nature of the interatomic forces in them. Since these elastic constants are functions of first and second order derivatives of the short range potential, their calculations will provide further check on the accuracy of short-range forces in these materials. Following Singh (1982) and subjecting the dynamical matrix within the framework of Shell model to the long wavelength limit, we find the expressions for the SOEC for *B3* phase as

$$C_{11} = L\left[\begin{array}{l} 0{\cdot}2477g + \frac{1}{3}(A_1 + 2B_1) \\ + \frac{1}{2}(A_2 + B_2) + 5{\cdot}8243Zg_1 \end{array}\right], \tag{6a}$$

$$C_{12} = L\left[\begin{array}{l} -2{\cdot}6458g + \frac{1}{3}(A_1 - 4B_1) \\ + \frac{1}{4}(A_2 - 5B_2) + 5{\cdot}8243g_1 \end{array}\right], \tag{6b}$$

$$C_{44} = L\left[\begin{array}{l} -0{\cdot}123g + \frac{1}{3}(A_1 + 2B_1) + \frac{1}{4}(A_2 + 3B_2) \\ -\frac{1}{3}\nabla(-7{\cdot}53912g + A_1 - B_1) \end{array}\right]. \tag{6c}$$

Henceforth, the expressions for pressure derivatives of SOEC follows

$$\frac{dS}{dP} = -(2\Omega)^{-1}\left[\begin{array}{l} -11{\cdot}5756\ g + 2(A_1 - 2B_1) + \frac{2}{3}A_2 \\ -\frac{7}{2}B_2 + \frac{1}{4}C_2 + 37{\cdot}5220\ Zg_2 \end{array}\right], \tag{7a}$$

$$\frac{dB_T}{dP} = -(3\Omega)^{-1}\left[\begin{array}{l} 20{\cdot}1788\,g - 3(A_1 + A_2) + 4(B_1 + B_2) \\ +3(C_1 + C_2) - 104{\cdot}8433\,Zg_1 \\ +22{\cdot}7008\,Zg_2 \end{array}\right], \tag{7b}$$

$$\frac{dC_{44}}{dP} = -(\Omega)^{-1}\left\{\left[\begin{array}{l} 0\cdot 4952g + \frac{1}{3}(A_1 - 4B_1 + C_1) \\ +\frac{1}{4}(2A_2 - 6B_2 - C_2) \\ +2\cdot 522Zg_2 + 4\cdot 9667Zg_1 \end{array}\right] + \nabla\left[\begin{array}{l} -17\cdot 5913g + A_1 - B_2 - \frac{2}{3}C_1 \\ +40\cdot 6461Zg_1 - 5\cdot 0440Zg_2 \end{array}\right] + \nabla^2\left[\begin{array}{l} 3\cdot 1416g + \frac{2}{3}(A_1 - B_2) \\ +\frac{C_1}{3} - 15\cdot 9412Zg_1 + 8\cdot 805Zg_2 \end{array}\right]\right\}. \tag{7c}$$

Furthermore, we have derived the expression for anharmonic third-order elastic constants (TOEC). Their relevant expressions are given below

$$C_{111} = L\left[\begin{array}{l} 0\cdot 5184g + \frac{1}{9}(C_1 - 6B_1 - 3A_1) \\ +\frac{1}{4}(C_2 - B_2 - 3A_2) - 2(B_1 + B_1) \\ -9\cdot 9326Zg_1 + 2\cdot 522Zg_2 \end{array}\right], \tag{8a}$$

$$C_{112} = L\left[\begin{array}{l} 0\cdot 3828g + \frac{1}{9}(C_1 + 3B_1 - 3A_1) + \frac{1}{8} \\ (C_2 + 3B_2 - 3A_2) - 11\cdot 642Zg_1 + 2\cdot 522Zg_2 \end{array}\right], \tag{8b}$$

$$C_{123} = L\left[\begin{array}{l} 6\cdot 1585g + \frac{1}{9}(C_1 + 3B_1 - 3A_1) \\ -12\cdot 5060Zg_1 + 2\cdot 5220Zg_2 \end{array}\right], \tag{8c}$$

$$C_{144} = L\left\{\begin{array}{l} 6\cdot 1585g + \frac{1}{9}(C_1 + 3B_1 - 3A_1) \\ -4\cdot 1681Zg_1 + 0\cdot 8407Zg_2 \\ +\nabla\left[-3\cdot 3507g - \frac{2}{9}C_1 + 13\cdot 5486Zg_1 - 1\cdot 681Zg_2\right] \\ +\nabla^2\left[\begin{array}{l} -1\cdot 5637g + \frac{2}{3}(A_1 - B_1) \\ +\frac{C_1}{9} - 5\cdot 3138Zg_1 + 2\cdot 9350Zg_2 \end{array}\right] \end{array}\right\}, \tag{8d}$$

$$C_{166} = L\left\{\begin{array}{l} -2\cdot 1392g + \frac{1}{9}(C_1 - 6B_1 - 3A_1) \\ +\frac{1}{8}(C_2 - 5B_2 - 3A_2) - (B_1 - B_2) \\ -4\cdot 168Zg_1 + 0\cdot 8407Zg_2 + \nabla\left[\begin{array}{l} -8\cdot 3768g + \frac{2}{3}(A_1 - A_2) \\ -\frac{2}{9}C_1 + 13\cdot 5486Zg_1 \\ -1\cdot 6813Zg_2 \end{array}\right] + \nabla^2\left[\begin{array}{l} 2\cdot 3527g + \frac{C_1}{9} - 5\cdot 3138Zg_1 \\ +2\cdot 9350Zg_2 \end{array}\right] \end{array}\right\}, \tag{8e}$$

$$C_{456} = L\left\{\begin{array}{l} 4\cdot 897g + \frac{1}{9}(C_1 - 6B_1 - 3A_1) \\ -B_2 + \nabla\left[-5\cdot 0261g - \frac{1}{9}C_1\right] \\ +\nabla^2\left[7\cdot 0580g + \frac{1}{3}C_1\right] \\ +\nabla^3\left[-4\cdot 8008g + \frac{1}{3}(A_1 - B_1) - \frac{1}{9}C_1\right] \end{array}\right\}. \tag{8f}$$

Various symbols appearing in the above equations are associated with the crystal energy and have the following form

$$A_1 = A_{ij} = L'\left(\frac{d^2}{dr^2}U_{ij}^{SR}(r)\right)_{r=r_0}, \tag{9a}$$

$$A_2 = A_{ii} = A_{jj} = L'\left(\frac{d^2}{dr^2}U_{ii}^{SR}(r) + \frac{d^2}{dr^2}U_{jj}^{SR}(r)\right)_{r=r_0}, \tag{9b}$$

$$B_1 = B_{ij} = \frac{L'}{a}\left(\frac{d}{dr}U_{ij}^{SR}(r)\right)_{r=r_0}, \tag{9c}$$

$$B_2 = B_{ii} = B_{jj} = \frac{L'}{a}\left(\frac{d}{dr}U_{ii}^{SR}(r) + \frac{d}{dr}U_{jj}^{SR}(r)\right)_{r=r_0}, \tag{9d}$$

$$C_1 = C_{ij} = L'a\left(\frac{d^3}{dr^3}U_{ij}^{SR}(r)\right)_{r=r_0}, \tag{9e}$$

$$C_2 = C_{ii} = C_{jj} = L'a\left(\frac{d^3}{dr^3}U_{ii}^{SR}(r) + \frac{d^3}{dr^3}U_{jj}^{SR}(r)\right)_{r=r_0}, \tag{9f}$$

$$g = Z + 8f(r), \tag{9g}$$

$$g_1 = r_0 df(r), \tag{9h}$$

$$g_2 = r_0 ddf(r), \tag{9i}$$

$$\nabla = \left[\frac{-7\cdot5391g + (A_1 - B_1)}{-3\cdot141g + (A_1 + 2B_1) + 21\cdot765g_1}\right], \tag{9j}$$

$$\Omega = -5\cdot0440g + (A_1 + A_2) - 2(B_1 + B_2) + 17\cdot4730Zg_1, \tag{9k}$$

$$B_T = \frac{1}{3}(C_{11} + 2C_{12}), \tag{9l}$$

and

$$S = \frac{1}{2}(C_{11} - C_{12}), \tag{9m}$$

in terms of the short-range energy

$$U_{ij}^{SR}(r) = bb_{ij}\exp\left(\frac{r_i + r_j - r_{ij}}{r}\right) - \frac{c_{ij}}{r_{ij}^6} - \frac{d_{ij}}{r_{ij}^8}, \tag{10}$$

with $L = (e^2/4a^4)$ and $L' = (4a^3/e^2)$. Having discussed the effective interionic potential, we now evaluate various thermodynamical and elastic properties for chosen material.

3. Results and discussion

The effective interionic potential described in the earlier section for zinc blende ($B3$) and rocksalt ($B1$) phases contains three free parameters, *viz*. the range (r), hardness (b) and three-body force parameters, $f(r)$. While estimating free parameters, we first deduce the van der Waals coefficients from the vibrational method (Slater and Kirkwood 1931) which are listed in table 1.

The values of these three free parameters have been determined by using the expressions for any two of the three elastic constants and lattice constant. The input data and model parameters are listed in table 2.

Considering pressure and temperature as the external variables (hydrostatic conditions), the free energy of a particular crystal structure at a particular temperature and pressure is obtained by minimizing G (P, V, T) with respect to V. In an attempt to reveal the structural phase transition of the test material, we minimize the Gibb's free energies, $G_{B3}(r)$ and $G_{B1}(r')$, for the equilibrium interatomic spacings (r) and (r'). As the pressure is increased, ΔG decreases and approaches to zero at the phase transition pressure. Beyond this pressure, ΔG becomes negative as the phase $B1$ is more stable. The Gibbs free energy difference, ΔG [$= G_{B3}(r) - G_{B1}(r')$], have been plotted as functions of pressure (P) in figures 1(a)–(c).

The pressure corresponding to ΔG approaching to zero is the phase transition pressure (P_t) of ZnSe [ZnS, ZnTe] and is about 13·5 [15, 9] GPa. The estimated value of P_t is consistent with that revealed from experiment, 13 [14·5, 9] GPa (Smith and Martin 1965; Nelmes and Mcmohan 1998). The consistency is attributed to the properly formulated effective interionic potential as well as use of free parameters. It is worth to point out that the uncertainties in the transition pressures can be as large as 10% or more. Quite generally, the experimental high-pressure measurements can suffer from several problems including calibration, inhomogeneous pressure, and metastability. Van Vechten (1973) briefly discussed these aspects, e.g. the role of metastability in pressure experiments.

Table 1. Van der Waals coefficients of ZnX (X = Se, S, Te) semiconductor (c_{ij} in units of 10^{-60} erg cm^6 and d_{ij} in units of 10^{-76} erg cm^8).

Sl. No.	vdW coefficients	ZnSe	ZnS	ZnTe
1.	c_{11}	38·04	38·04	38·04
2.	c_{12}	112·81	98·88	149·11
3.	c_{22}	533·96	384·42	1087·31
4.	C	709·24	591·59	1078·19
5.	d_{11}	12·07	12·07	12·07
6.	d_{12}	115·26	90·03	197·00
7.	d_{22}	702·23	453·11	1812·47
8.	D	586·33	445·34	1100·3

Table 2. Input data and model parameter (C_{11}, C_{12} and C_{44} are elastic constants in units of 10^{11} Nm^{-2}), a is lattice constant for units 10^{-8} cm, b and r are the hardness parameter and range in the units 10^{-12} erg (10^{-8} cm).

	Input data				Model parameters		
Solid	a	C_{11}	C_{12}	C_{44}	b	r	$f(r)$
ZnS	2·705[a]	10·40[a]	6·50[a]	4·62[a]	1·102	3·53	– 0·00747
ZnSe	2·835[a]	8·59[a]	5·06[a]	4·06[a]	1·072	3·22	– 0·0011
ZnTe	3·050[a]	7·11[a]	4·07[a]	3·12[a]	1·319	3·54	– 0·0080

[a]Lee (1970).

We now estimate values of the relative volume associated with various compressions following Murnaghan equation of state (Singh 1982)

$$\frac{V}{V_0} = \left(1 + \frac{B'}{B_0} P\right)^{-1/B'}, \tag{11}$$

V_0 being the cell-volume at ambient conditions. Following the estimated values of pressure dependent radius for both the structures, the curve of volume collapse with pressure to depict the phase diagram are illustrated in figures 2(a)–(c). It is noticed from the plots that our approach has predicted correctly the relative stability of competitive crystal structures, as the values of ΔU are positive.

In order to study the high-pressure elastic behaviour of ZnX, we have computed the second-order elastic constants (SOEC) and their variation with pressure is shown in figures 3(a)–(c). We note that C_{44} decreases linearly with the increase of pressure away from zero at the phase-

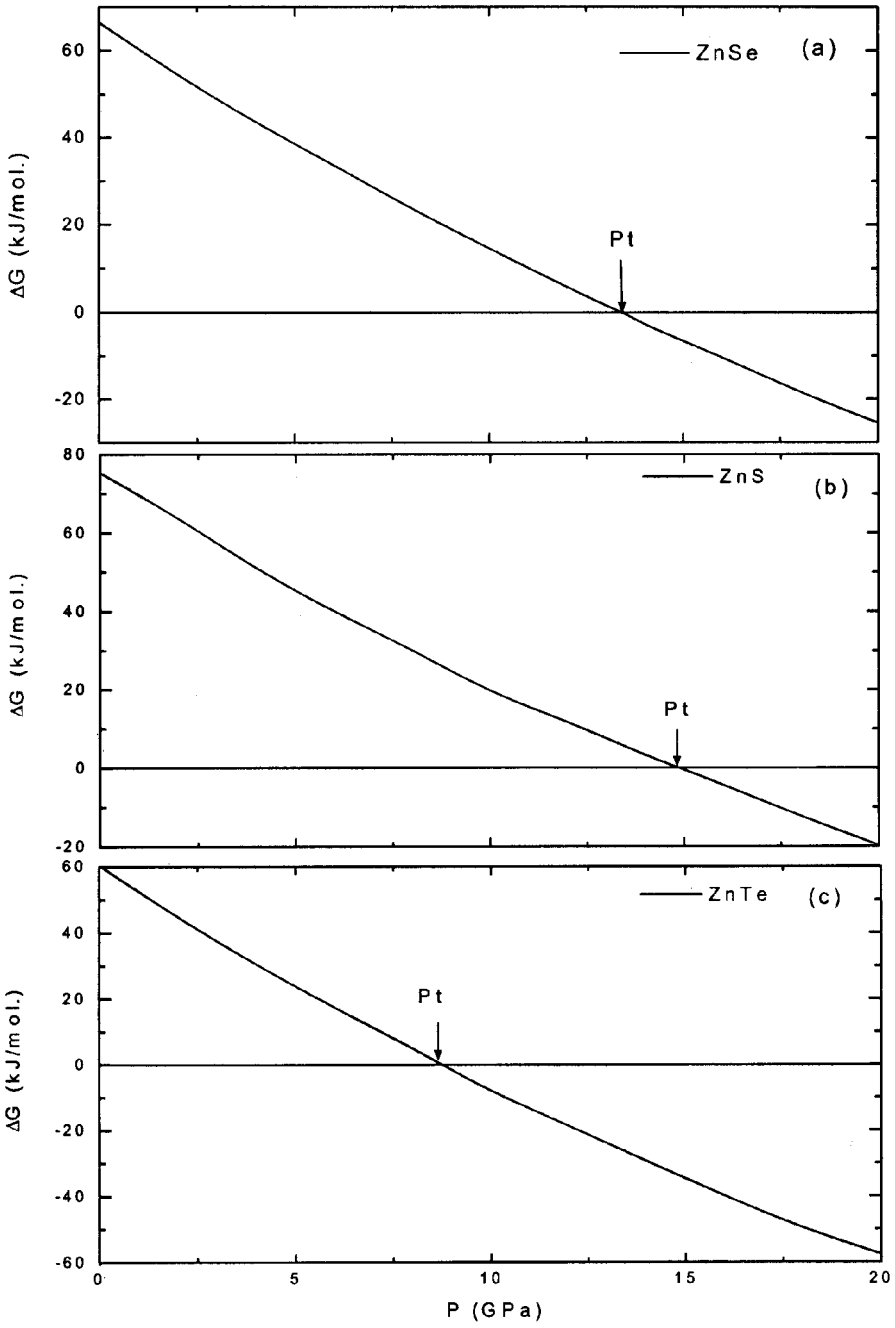

Figure 1. Variation of Gibbs free energy difference with pressure.

transition pressures. This feature is in accordance with the first-order character of the transition for all the compounds and is similar to that earlier reported in the cases of HgTe (Se) (Miller *et al* 1981; Ford *et al* 1982). On the contrary, values of C_{11} and C_{12} increase linearly with pressure and resemble that observed in HgTe (Se).

It is instructive to mention that the Born criterion for a lattice to be mechanically stable is that the elastic energy density must be a positive definite quadratic function of strain. This requires that the principal minors (alternatively the eigenvalues) of the elastic constant matrix should all be positive. The stability of a cubic crystal is expressed in terms of elastic constants as follows: $B_T = [C_{11} + 2C_{12}]/3 > 0$, $C_{44} > 0$ and $s = [C_{11}–C_{12}]/2 > 0$. Here, C_{ij} are the conventional elastic constants and B_T the bulk modulus. The quantities, C_{44} and s, are shear and

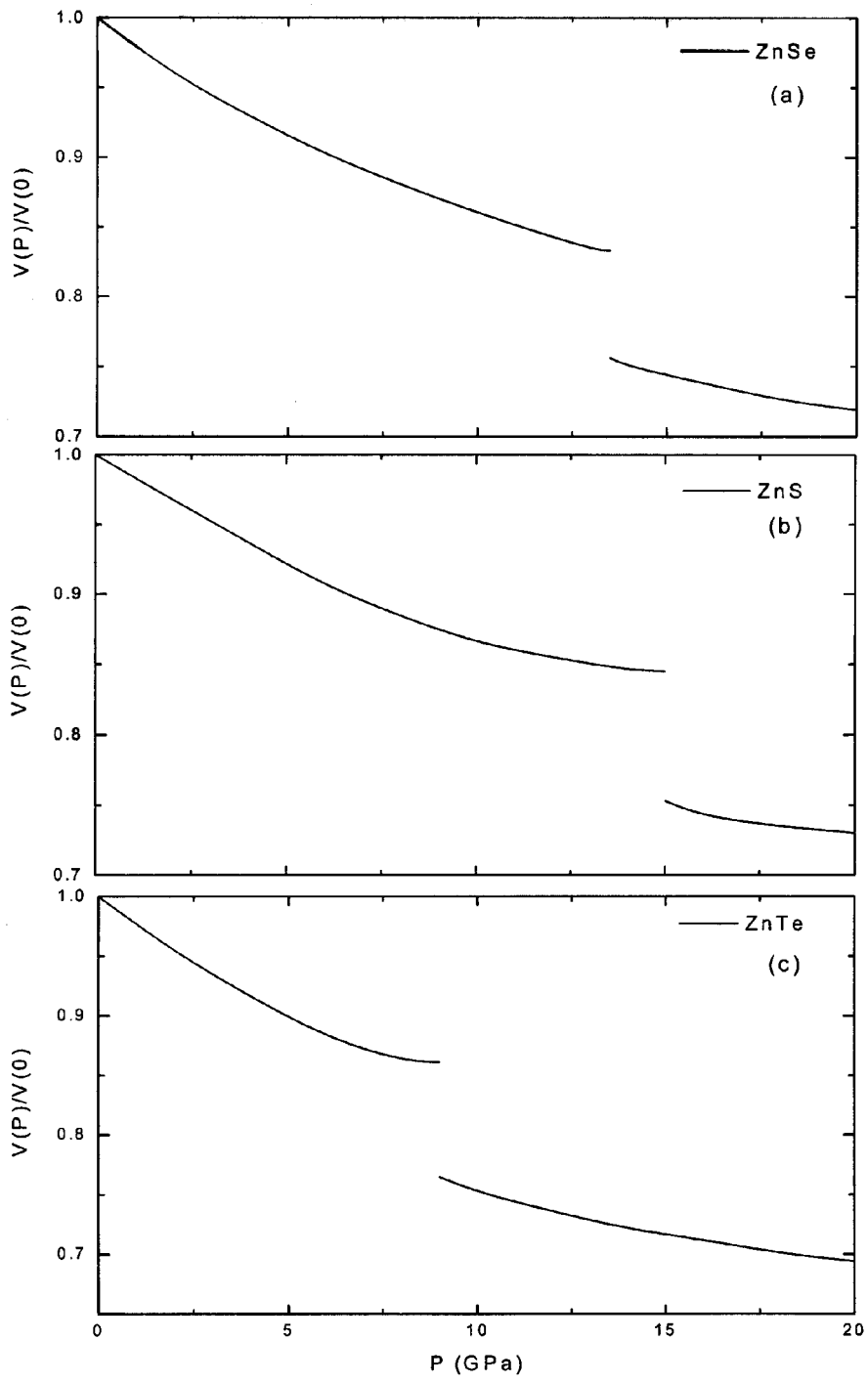

Figure 2. Phase diagram of ZnX [X = S, Se, Te].

tetragonal moduli of a cubic crystal. Estimated values of bulk modulus of ZnSe (ZnS, ZnTe) are B_T = 0·95 (1·1, 0·75) 10^{11} Nm^{-2} and shear moduli, C_{44} = 0·72 (0·85, 0·55) 10^{11} Nm^{-2} and tetragonal moduli, s = 0·20 (0·23, 0·15) 10^{11} Nm^{-2} well satisfied the above elastic stability criteria. In addition, Vukcevich (1972) proposed a high-pressure stability criterion for ionic crystals, combining mechanical stability with minimum energy conditions. In accordance, the stable phase of a crystal is one in which the shear elastic constant, C_{44}, is nonzero (for mechanical stability) and which has the lowest potential energy among the mechanically stable lattices. Also, the pressure at which C_{44} = 0 (i.e. shear instability) indicates the upper bound for the transition pressure. Thus, it is inferred from

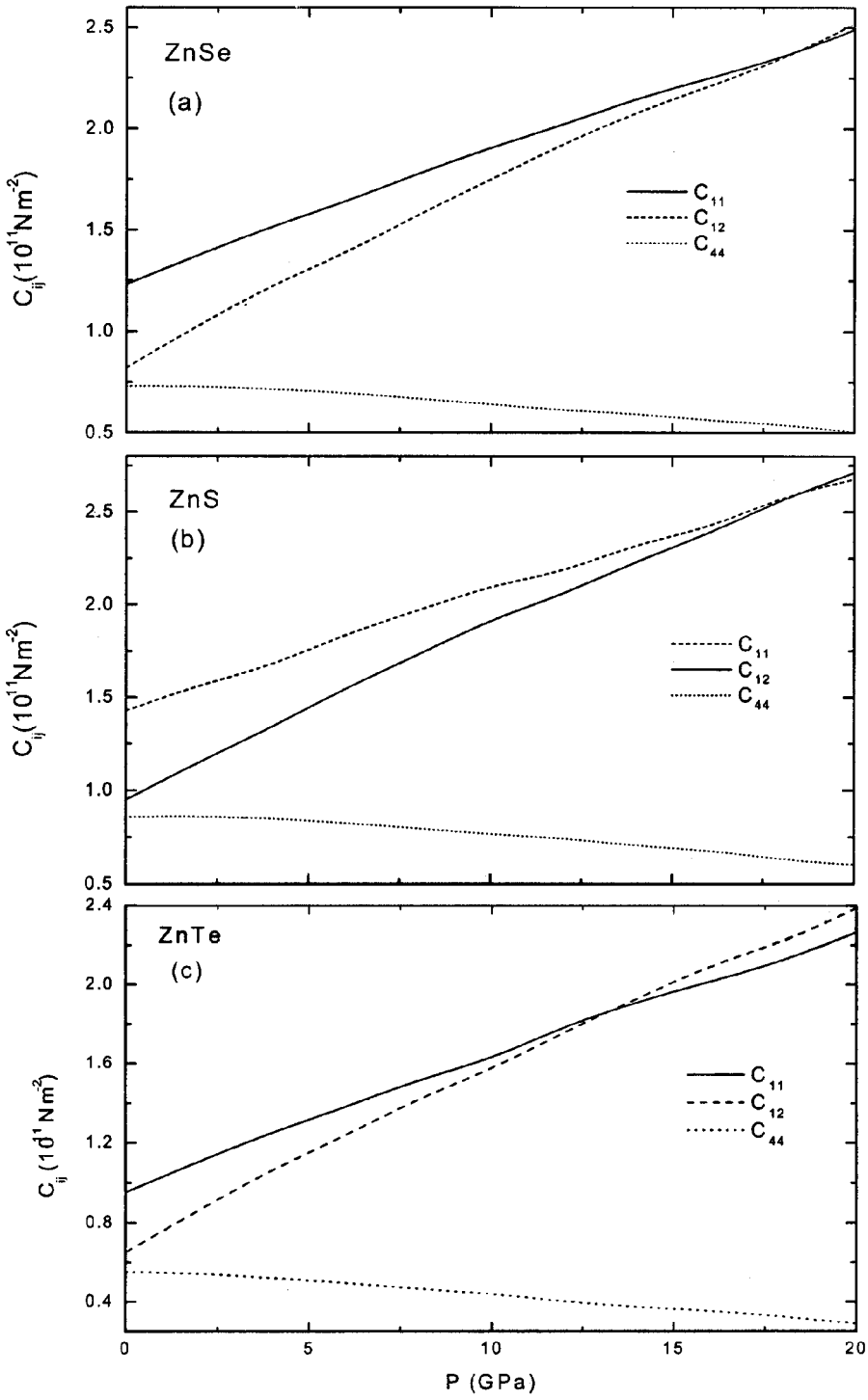

Figure 3. Variation of second order elastic constants with pressure.

figures 1 and 3 that the shear instability is higher than the corresponding transition pressure. This supports the high-pressure stability criterion proposed by Vukcevich (1972).

It is also our objective to reveal the anharmonic properties of ZnX by computing the pressure derivatives of SOEC at zero pressure and third-order elastic constants (TOEC). We have, therefore, deduced the values of pressure derivatives which are listed in table 3 along with available experimental data. It is true that the agreement between the theoretical and the experimental value of dC_{44}/dP is not of the desired degree but this may be because we have derived our expressions neglecting thermal effects and assuming the overlap repulsion significant only up to nearest neighbours.

In continuation, the variations of TOEC with pressure are shown in figures 4(a)–(c). These points reveal that the values of C_{111}, C_{112}, C_{123}, C_{166} and C_{456} are negative, while that of C_{144} is positive as obtained from the effective interionic potential at zero pressure. Furthermore, C_{166} and C_{144} increase, on the other hand, remaining TOEC decreases with pressure and follows a systematic trend. Experimental studies on the TOEC of the system of solids under consideration are relatively difficult and the only measurements available up to date are on the pressure derivatives of the SOE constants.

Apart from elastic constants, we have investigated various important physical properties like force constant (f), Debye temperature (q_D), Gruneisen parameter (g), Reststrahlen frequency (n_0), compressibility (b) and pressure derivative of bulk modulus (B_T). The relevant expressions (Varshney *et al* 2004) used in our calculations are given below. The molecular force in the absence of the Lorentz effective field is given by

$$f = \frac{1}{3}\left[\frac{d^2}{dr^2}U_{SR}(r) + \frac{2}{r_0}\frac{d}{dr}U_{SR}(r)\right]_{r=r_0}, \tag{12}$$

which consists of the SR overlap repulsion and the van der Waals interaction potentials between the unlike ions. The force constant in turn gives the Reststrahlen frequency as

$$n_0 = \frac{1}{2p}\left[\frac{f}{m}\right]^{1/2}, \tag{13}$$

with m being the reduced mass.

The Debye temperature is written as

$$q_D = \hbar n_0 / k. \tag{14}$$

Table 3. ZnX with zinc blende structure.

Solid	dK/dP	dS/dP	dC_{44}/dP
ZnS	5·12 (4·9)[a]	– 0·50	1·14
ZnSe	4·86 (4·77)[b]	– 0·39 (– 0·12)[b]	1·13 (0·43)[b]
ZnTe	5·16 (5·04)[b]	– 0·44 (– 0·08)[b]	0·95 (0·45)[b]

[a]Madelung *et al* (1982); [b]Lee (1970).

In order to describe the anharmonic properties, we have calculated g from the relation

$$g = -\frac{r_0}{6}\left[\frac{U'''(r_0)}{U''(r_0)}\right], \tag{15}$$

and the compressibility

$$b = \frac{r_0^2}{9V}[U''(r_0)]. \tag{16}$$

The above thermodynamic parameters are listed in table 4. We have used the effective interionic potential to predict successfully the elastic and anharmonic properties of semiconducting compounds under consideration. It is noticed from table 4 that there exists substantial difference in the model calculated force constant and Reststrahlen frequency for ZnSe with the Raman scattering measurements data of Chou *et al* (1998) and eight-parameter bond-bending force model (Kushwaha and Kushwaha 1980). The above is due to the fact that in the present lattice model calculations, we consider the overlap repulsive potential only up to the second nearest neighbour. Also the developed effective interionic potential (EIOP) does not incorporate the thermal effects at finite temperature. These issues are of importance and need detailed investigations. Thus we do not claim the process to be rigorous, but a consistent agreement following EIOP is obtained on Debye temperature as those revealed from heat capacity measurements. Quite generally, the Debye temperature is also a function of temperature and varies from technique to technique and depends on the sample quality with a standard deviation of about 15 K. It is arguable that the deduced values of g are consistent with the Raman scattering measurements (Arora *et al* 1988) and the calculated g from the knowledge of phonon frequencies (long-wavelength phonons) as a function of the crystal volume (Adachi 2005). This can be attributed to the proper incorporation of various interactions in the effective interionic potential.

The Debye temperature (q_D), from the present approach, can be redefined in terms of SOEC

$$q_D^3 = \frac{3\cdot15}{8p}\left(\frac{h}{k_B}\right)^3\left(\frac{r}{M}\right)^{3/2}(C_{11}-C_{12})^{1/2}$$
$$(C_{11}+C_{12}+2C_{44})^{1/2}C_{44}^{1/2}, \tag{17}$$

where M is the acoustic mass of the compound and is plotted in figure 5 along with the available experimental data at zero pressure. One can approximate that this result motivates the definition of an 'average' elastic constant as

$$C = \left(\frac{8p}{3\cdot15}\right)^{2/3}\left(\frac{k_B}{h}\right)^2\left(\frac{M}{r}\right)q_D^2, \tag{18}$$

which in turn is calculated from the Debye temperature to allow us to correlate Cauchy discrepancy in elastic constant following

$$C^* = \frac{C_{12} - C_{44}}{C_{12} + C_{44}}, \tag{19}$$

at zero pressure. Figure 6 shows variation of average elastic constant (C) with Cauchy discrepancy (C^*) for ZnX compounds. It is worth to mention that C_{44} is larger as compared to C_{12}, which is consistent with the available experimental data on PbTe and SnTe possessing the NaCl structure with $B1$ to $B2$ structural phase transition. However, we note that the diluted magnetic semiconductors with zinc blende structure ($B3$ to $B1$ structural phase transition) and most of the body centred cubic transition metals show a positive Cauchy deviation, C^*.

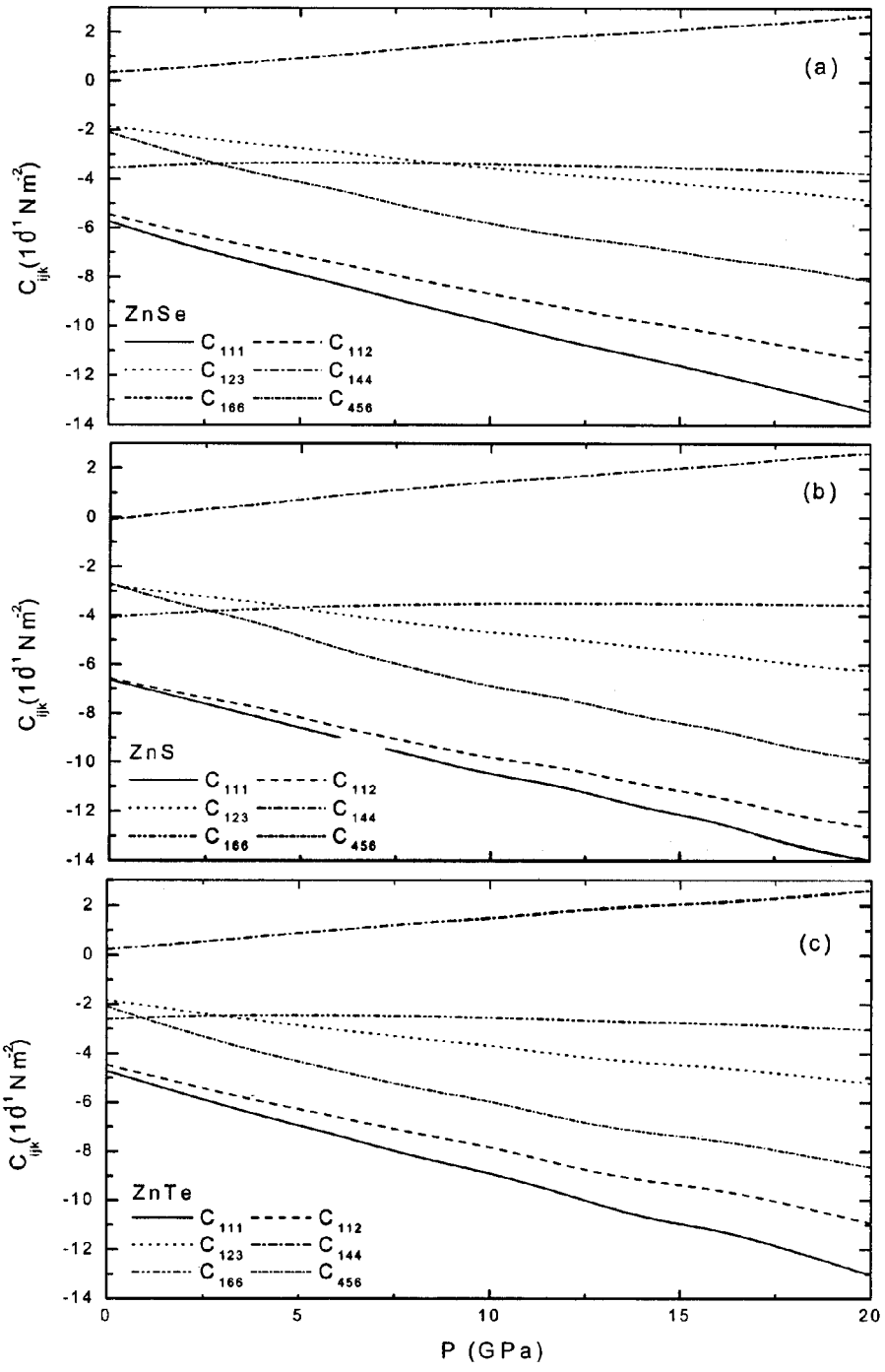

Figure 4. Variation of third order elastic constants with pressure.

Table 4. Thermodynamical properties of ZnX with zinc blende structure.

Properties	Formula	Calculated values			Reported data		
		ZnSe	ZnS	ZnTe	ZnSe	ZnS	ZnTe
Force constant (f) (10^5 dyne/cm)	20	2·114	2·292	1·723	4·59[a]		
Reststrahlen frequency (n_0) (10^{12} Hz)	21	1·806	2·426	1·483	6·42[b]	8·20[b]	5·20[b]
Debye temperature (q_D) (K)	22	371	544	320	400[c]	530[c]	223[c]
Gruneisen parameter (g)	23	1·98	2·042	2·1	1·55[d]	1·52[e]	1·58[e]
Compressibility (b) (10^{-11} Pa^{-1})	25	1·482	1·091	1·768			

[a]Chou *et al* (1998); [b]Kushwaha and Kushwaha (1980), Kushwaha (1981); [c]Lide (1999); [d]Arora *et al* (1988); [e]Adachi (2005).

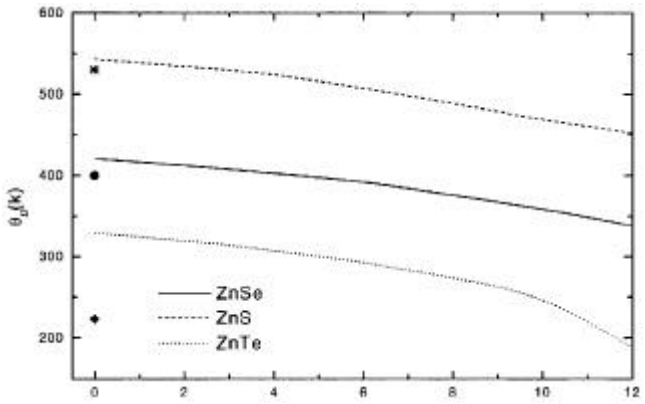

Figure 5. Variation of Debye temperature (q_D) with pressure. Closed cricle, star and diamond are the experimental data for ZnSe, ZnS and ZnTe at zero pressure.

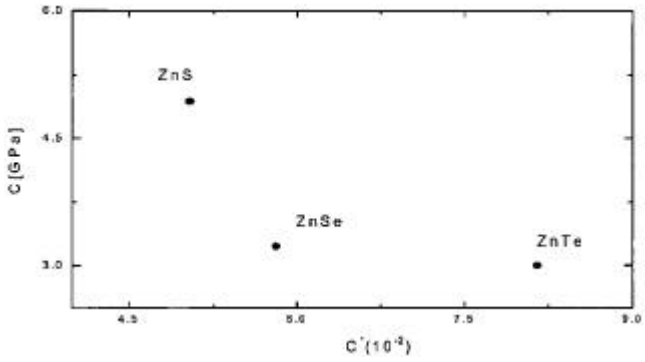

Figure 6. Shows 'average' elastic constant, C, as a function of Cauchy discrepancy, C^*, for ZnX compounds.

We finish by stating that the effective interionic potential consistently explains the high pressure, anharmonic behaviour and associated thermodynamic variables of the ZnX semiconducting compounds.

4. Conclusions

In the present investigation, an effective interaction potential is formulated in analysing the mechanical properties as well as anharmonicity in II–VI semiconductors. The obtained values of free parameters allow us to predict phase transition pressure and associated volume collapse. It is believed that vast volume discontinuity in pressure volume phase diagram identifies the structural phase transition from ZnS to NaCl structure. In continuation we explore our efforts to check the validity of Born criterion by computing the second order elastic constants that support high-pressure structural stability of binary ZnX semiconductors. It is noticed that C_{44} decreases linearly with increase of pressure and does not tend to be zero at the phase transition pressures. This feature is in accordance with the first order character of the transition. The above analysis reveals that the deviation from the experimental values of pressure derivative of elastic constant, C_{44}, is attributed to the fact that we have neglected the thermal effects and assuming the overlap repulsion significant only up to nearest neighbour.

We note that the variation of third order elastic constants with pressure points to the fact that the values of C_{111}, C_{112}, C_{123}, C_{166}, C_{456} are negative while that of C_{444} is positive as obtained from the effective interionic potential at zero pressure. The present study also presents a quantitative description of the physical thermodynamical parameters of the chosen semiconducting compound, ZnX, and tests the appropriateness of the effective interionic potential.

Acknowledgement

Financial assistance from the Defence Research Development Organization (DRDO), New Delhi, is gratefully acknowledged.

References

Adachi S 2005 *Properties of groups IV, III–V and II–VI semiconductors* (England: John Wiley and Sons) **87**

Arora A K, Suh E-K, Debska U and Ramdas A K 1988 *Phys. Rev*. **B37** 2927

Born M and Mayer J E 1932 *Z. Phys*. **75** 1

Chou W C *et al* 1998 *Chinese J. Phys*. **36** 120

Ford P J, Miller A J, Saunders G A, Yogurtcu Y K, Furdyna J K and Jaczynski M 1982 *J. Phys.* **C15** 657
Hafemeister D W and Flygare W H 1965 *J. Chem. Phys.* **43** 795
Jain Mukesh 1991 *Diluted magnetic semiconductors* (Singapore: World Scientific)
Kushwaha M S 1981 *Phys. Rev.* **B24** 2115
Kushwaha M S and Kushwaha S S 1980 *J. Phys. Chem. Solids* **41** 2115
Lee B H 1970 *J. Appl. Phys.* **41** 2988
Lide D R (ed.) 1999 *CRC handbook of chemistry and physics* (New York: CRC Press) **79** pp 12–93
Madelung O *et al* 1982 *Physics of II–VII and I–VII compounds semimagnetic semiconductors* (Berlin: Springer-Verlag) Landolt-Bornstein New Series, Group III, **Vol. 17b**
Miller A J, Saunders G A and Yogurtcu Y K 1981 *Philos. Mag.* **A43** 1447
Mujica A, Rubio A, Munoz A and Needs R J 2003 *Rev. Mod. Phys.* **75** 863
Nelmes R J and Mcmohan M I 1998 *Semicond. Semimetals* **54** 145
Piermarini G J and Block S 1975 *Rev. Sci. Instrum.* **46** 973
Singh R K 1982 *Phys. Reports* (*Netherlands*) **85** 259
Slater J C and Kirkwood J G 1931 *Phys. Rev.* **37** 682
Smith P L and Martin J E 1965 *Phys. Lett.* **19** 541
Tosi M P 1964 *Solid State Phys.* **16** 1
Tosi M P and Fumi F G 1962 *J. Phys. Chem. Solids* **23** 359
Van Vechten J A 1973 *Phys. Rev.* **B7** 1479
Varshney D *et al* 2004 *Phase Transition* **77** 1075
Vukcevich M R 1972 *Phys. Status Solidi* **b54** 435